Arabian Journal of Chemistry (2012) **5**, 353–359

King Saud University

Arabian Journal of Chemistry

www.ksu.edu.sa
www.sciencedirect.com

ORIGINAL ARTICLE

Adsorption of Cu^{2+} from aqueous solution onto iron oxide coated eggshell powder: Evaluation of equilibrium, isotherms, kinetics, and regeneration capacity

Rais Ahmad *, Rajeev Kumar, Shaziya Haseeb

Environmental Research Laboratory, Department of Applied Chemistry, Aligarh Muslim University, Aligarh 202002, India

Received 20 August 2010; accepted 9 September 2010
Available online 17 September 2010

KEYWORDS

Coating;
Adsorption;
Cu^{2+};
Kinetics;
Regeneration

Abstract This study explored the adsorption behavior of Cu^{2+} onto iron oxide coated eggshell powder (IOESP) from aqueous solution. The effect of various operational parameters such as pH, contact time, initial adsorbate concentration, surfactant, and temperature on adsorption of Cu^{2+} ions was investigated using batch adsorption experiments. The optimum pH for Cu^{2+} adsorption was found to be 6.0. Kinetics of adsorption was found to follow the pseudo-second-order rate equation. The suitability of Langmuir and Freundlich adsorption models to the equilibrium data was investigated. The adsorption was well described by the Freundlich isotherm model indicating the presence of heterogeneous sites for Cu^{2+} adsorption. The adsorption of Cu^{2+} was increased in the presence of anionic surfactant (SDS) while cationic surfactant (CTAB) shows no significant change in adsorption capacity. Thermodynamic parameters showed that the adsorption of Cu^{2+} onto IOESP was feasible, spontaneous, and exothermic. Regeneration studies were performed using HCl, HCOOH, EDTA, and NaOH as eluting agent for Cu^{2+} desorption from saturated IOESP and the maximum regeneration was observed with HCl.

1. Introduction

Copper is considered as one of the most toxic metal and poses a potential threat to the human health and environment, even at low concentrations. It has been well reported that the accumulation of copper in human body causes brain, skin, pancreas and heart diseases (Veli and Alyuz, 2007). The permissible limit of copper is 2.5 mg/L in water. Wastewater from various industries, such as electroplating, plastic, metal finishing, pigments, and mining contains copper. To alleviate the problem of water pollution by copper, various methods have been used to remove copper from wastewater such as chemical precipitation, coagulation, floatation, adsorption, ion exchange, reverse osmosis, and electrodialysis (Ali and

* Corresponding author. Address: Department of Applied Chemistry, Faculty of Engineering and Technology, Aligarh Muslim University, Aligarh 202002, India. Tel.: +91 0571 2700920 23x3000; fax: +91 0571 2400528.
E-mail address: olifiaraju@gmail.com (R. Ahmad).

Peer review under responsibility of King Saud University.
doi:10.1016/j.arabjc.2010.09.003

Production and hosting by Elsevier

Gupta, 2007; Soliman et al., 2010; Barakat, 2010). The production of the sludge in the precipitation method poses challenges in handling, treating, and land-filling of the solid sludge. Ion exchange usually requires a high-capital investment for the equipment as well as high operational cost. Electrolysis allows the removal of metal ions with the advantage that there is no need for additional chemicals and also there is no sludge generation. However, it is inefficient at a low metal concentration. Membrane processes such as reverse osmosis and electrodialysis tend to suffer from the instability of the membranes in salty or acidic conditions and fouling by inorganic and organic substances present in wastewater (Dang et al., 2009a,b).

Adsorption is highly effective, economical, promising, and is widely applied for scavenging the metal bearing wastewaters. Different conventional and non-conventional adsorbents have been used for the removal of heavy metals (Gupta et al., 2009; Gupta and Rastogi, 2009). Hen eggshell is the one of the major by product of the food industry. The by-product eggshell weighs approximately 10% of the total mass (≈60 g) of hen egg, representing a significant waste from the egg-derived products processor because it was traditionally useless and commonly disposed of in landfills without any pretreatment (Stadelman, 2000; Tsai et al., 2008). Hen eggshell typically consists of ceramic materials constituted by a three-layered structure, namely the cuticle on the outer surface, a spongy (calcareous) layer and an inner lamellar (or mammillary) layer (Tullett 1987; Stadelman, 2000; Tsai et al., 2006). The chemical composition (by weight) of by-product eggshell has been reported as follows: calcium carbonate (94%), magnesium carbonate (1%), calcium phosphate (1%), and organic matter (4%) (Stadelman, 2000). Due to its large production, the use of hen eggshell as adsorbents has slightly increased in recent years. Chojnacka (2005) studied the adsorption of Cr(III) ions from aqueous solutions using crushed hen eggshells, and found that they had a relatively high sorption capacity as compared to other adsorbents. Vijayaraghavan et al. (2005) investigated the adsorption capacity of crushed eggshell for removal of copper ions from aqueous solutions by column process. Otun et al. (2006) reported adsorption of Pb(II), Ni(II), and Cd(II) ions from aqueous solutions using powdered eggshell.

In this work, eggshell powder surface was modified by the coating of iron oxide. Iron oxides are effective in metal removal owing to the high affinity between iron oxides and metal species (Lim et al., 2008; Sharma and Srivastava, 2010; Zhang et al., 2010). The adsorption characteristics of iron oxide coated eggshell powder (IOESP) have been systematically studied in batch as a function of contact time, pH, metal ion concentration, and temperature. Kinetic measurements were assessed at different Cu^{2+} concentrations and evaluated by the pseudo-first order, pseudo-second order, and intraparticle diffusion model.

2. Materials and methods

2.1. Materials

$FeSO_4{\cdot}7H_2O$ was purchased from Qualigens Fine Chemicals. *N*-Cetyl-*N*,*N*,*N*-trimethyl ammonium bromide (CTAB), HCl, HCOOH, NaOH, sodium dodecyl sulfate (SDS), and $Cu(NO_3)_2$, $Pb(NO_3)_2$, $Ni(NO_3)_2$ were obtained from CDH Ltd., India. Metal ion solutions were prepared by dissolving appropriate amount of metal salt in double distilled water.

2.2. Equipments

The concentration of Cu^{2+} in the aqueous solution was analyzed using atomic absorption spectroscopy (AAS) (GBC 902, Australia). The FTIR spectra of IOESP before and after Cu^{2+} adsorption were recorded in the frequency range of 400–4000 cm^{-1} using FTIR spectrophotometer (Inter-spec 2020, Spectro lab, UK) in KBr pellets. pH measurements were made using a pH meter (Elico LI-120, India).

2.3. Preparation of iron oxide coated eggshell powder

Hen eggshell waste was washed with distilled water and dried at 100 °C. Dried waste shell was crushed and converted to a fine powder of 100 BSS mesh particles. The fine eggshell powder was washed several times with distilled water and dried at 100 °C. Then 10 g eggshell powder immersed in 50 mL solution of $FeSO_4{\cdot}7H_2O$ (10 g) and 20 mL 5 N NaOH solution was added drop wise to precipitate the iron oxide on the surface of the eggshell powder. The solution was continuously stirred for 1 h. After that, iron oxide coated eggshell powder was filtered, washed several times and dried at 100 °C.

2.4. Determination point of zero charge (pHz)

The point of zero charge (pHz) was to be investigated to find the surface charge of IOESP. For the determination of pHz, 0.1 M KCl was prepared and its initial pH was adjusted between 2.0 and 12.0 by using NaOH and HCl. Then, 25 mL of 0.1 M KCl was taken in the 100 mL flasks and 0.05 g of IOESP was added to each solution. These flasks were kept for 24 h and the final pH of the solutions was measured by using a pH meter. Graphs were plotted between pH_{final} and $pH_{initial}$ (Sharma et al., 2009).

2.5. Batch adsorption studies

2.5.1. Metal selectivity study

The selective nature of IOESP was studied for Cu^{2+}, Pb^{2+}, and Ni^{2+}. The IOESP shows the affinity for the metal ions as follows $Cu^{2+} > Pb^{2+} > Ni^{2+}$. On the basis of this primary study, Cu^{2+} was selected for a detailed adsorption study.

2.5.2. Kinetic studies

Batch kinetic experiments were performed by mixing 0.05 g adsorbent to each conical flask with 25 mL of metal ion solution of 50 and 100 mg L^{-1} concentration at 30 °C. A series of such conical flasks were then shaken at a constant speed of 80 rpm in a water bath shaker and samples were collected at different time intervals. The concentration of Cu^{2+} in the supernatant solution was analyzed using AAS. The equilibrium adsorption capacity of IOESP for Cu^{2+} was calculated from the relationship:

$$q_e = (C_0 - C_e)V/M \quad (1)$$

where q_e is the equilibrium adsorption capacity (mg g^{-1}), C_e is the metal ion concentration (mg L^{-1}) at equilibrium, V is the volume (L) of solution, and M is the weight (g) of adsorbent.

2.5.3. Equilibrium studies

The effect of the initial metal ion concentration was determined by placing 0.05 g of the adsorbent in 25 mL of metal ion solution of different initial concentrations (10–100 mg L^{-1}) for 180 min at 30 °C. The concentration of Cu^{2+} left in supernatant solution was determined by AAS.

2.5.4. Effect of pH on Cu^{2+} adsorption

The influence of solution pH on the Cu^{2+} adsorption was studied over the pH range from 2 to 6. The pH was adjusted using 0.1 M HCl and NaOH solutions. In this study, 25 mL of Cu^{2+} solution of 50 and 100 mg L^{-1} were agitated with 0.05 g of IOESP for 180 min at 30 °C. In the subsequent investigations, experiments were performed at solution pH value up to 6 to avoid any possible hydroxide precipitation.

2.5.5. Desorption studies

Desorption studies were performed in batch using 0.01 M and 0.1 M of HCl, HCOOH, EDTA, and NaOH. 25 mL Cu^{2+} solution of 100 mg L^{-1} metal ion concentration was treated separately with 0.05 g of adsorbent. The adsorbent in each flask was washed several times with distilled water to remove excess of metal ions. Then Cu^{2+} saturated adsorbent was agitated with 25 mL eluent for 180 min. The amount of Cu^{2+} desorbed in the eluent solution was analyzed by AAS.

3. Results and discussion

3.1. Effect of pH

The pH value of the solution plays an important role in the adsorption of Cu^{2+} on IOESP. The adsorption of Cu^{2+} onto IOESP increases with increasing solution pH (Fig. 1). Similar results were also reported for Cu^{2+} adsorption on iron pillared montmorillonite (Li and Wua, 2010) and on Al_2O_3 (Wua et al., 2003). The effect of pH may be explained in terms of zero point of charge (pHz) of the adsorbent (pHz of IOESP is 7.9, Fig. 1 inset), at which the adsorbent is neutral. The surface charge of the adsorbent is positive when solution pH is below pHz. An increase in pH above pHz will show a slight increase in adsorption as long as the metal species are still positively charged or neutral even though the surface of the adsorbent is negatively charged. When both the surface charge of the adsorbent and metal species charge become negative, the adsorption will decrease significantly. Decrease in removal of metal ions at lower pH is apparently due to the higher concentrations of H^+ in the solution, which compete with Cu^{2+} ions for the adsorption sites of IOESP. Generally, the positive charge of the adsorbent surface decreases with the increasing pH value, leading to the decrease in the repulsion between the adsorbent surface and Cu^{2+}, thus improving the adsorption capacity (Gupta, 1998).

3.2. Adsorption kinetics

The adsorption kinetics of IOESP for Cu^{2+} at 30 °C is shown in Fig. 2 and the adsorption was quick in the beginning and then slow. The adsorption equilibrium was established in about 180 min. After this period, the amount of adsorbed metal ions did not change significantly with time. The rapid uptake of metal ions onto IOESP may indicate that most of reaction sites of the adsorbent are exposed for interaction with metal ions. Furthermore, due to the presence of hydroxyl group in adsorbent, complexation may occur between metal ion and adsorbent surface which significantly shows fast adsorption (Gupta et al., 2010a).

To determine the kinetics of adsorption of Cu^{2+} on IOESP, pseudo-first-order, pseudo-second-order and intraparticle diffusion models were applied. The pseudo-first-order model is given by:

$$\log(q_e - q_t) = \log q_e - k_1 t/2.303 \quad (2)$$

where k_1 is the pseudo-first-order rate constant (min^{-1}) and q_e (mg g^{-1}) is the adsorption capacity at equilibrium and q_t (mg g^{-1}) is the amount of metal adsorbed at any time t. On the other hand pseudo-second order model is expressed as:

$$t/q_t = (1/k_2 q_e^2) + t/q_e \quad (3)$$

where k_2 (g mg^{-1} min^{-1}) is the pseudo-second-order rate constant. The values of q_e, k_1 and k_2 for different concentrations were calculated from their respected plots (figure not shown) and the results are shown in Table 1. It can be seen that the values of correlation coefficient for pseudo-second-order are

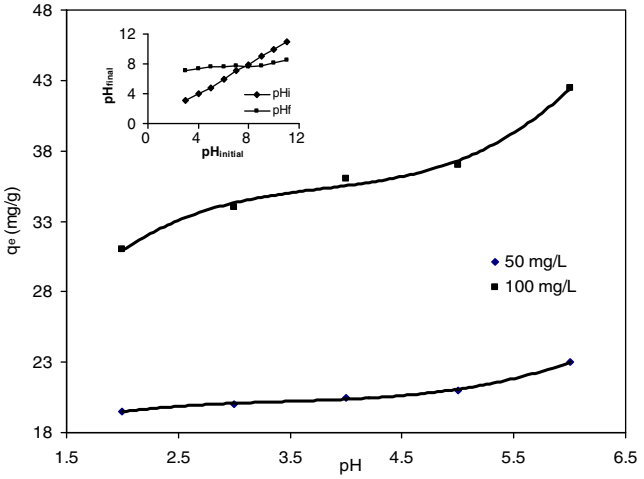

Figure 1 Effect of pH on Cu^{2+} adsorption on IOESP. Determination of pHz of IOESP (inset).

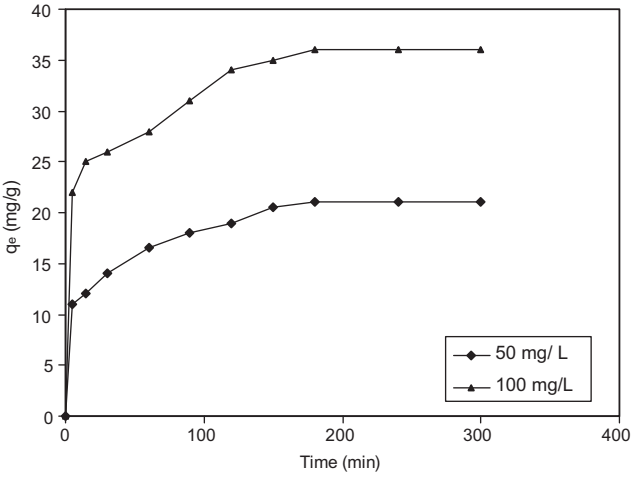

Figure 2 Effect of contact time on Cu^{2+} adsorption onto IOESP.

Table 1 Kinetic parameters for the adsorption of Cu^{2+} onto IOESP.

Conc. (mg L^{-1})	q_e (exp) (mg g^{-1})	Pseudo-first-order			Pseudo-second-order			Intraparticle diffusion	
		q_e	k_1	R^2	q_e	k_1	R^2	k_{id}	R^2
50	21	12.56	0.018	0.9330	21.97	0.003	0.9923	0.742	0.9246
100	36	15.80	0.015	0.9348	37.17	0.002	0.9924	1.018	0.9289

relatively higher than those for pseudo-first-order kinetic model. Additionally, experimental q_e values are very close to the calculated q_e values for pseudo-second-order kinetic model. These results implied that the adsorption of Cu^{2+} could be best described by the pseudo-second order model (Gupta et al., 2010b). As shown in Table 1, the value of rate constant k_2 decreases with increasing initial concentration and surface loading. Higher surface loadings would result in less diffusion efficiency and a high competition of metal ions for fixed reaction sites, consequently lower k_2 values were observed.

Intraparticle diffusion can be estimated by using the Weber–Morris intraparticle diffusion model

$$q_t = k_{id} t^{1/2} + C \tag{4}$$

where k_{id} (g mg^{-1} $min^{-1/2}$) is the intraparticle diffusion rate coefficient and C gives an idea about the thickness of the boundary layer. These values were determined by a plot of q_t versus $t^{1/2}$ (figure not shown) and the straight lines deviated from the origin. The difference between final mass transfer rate and initial mass transfer rate may cause the deviations of the straight lines. Also, this deviation can show that the pore diffusion is not the sole rate-controlling step. The k_{id} values are shown in Table 1.

3.3. Adsorption isotherms

The adsorption of Cu^{2+} onto IOESP at 30 °C was determined as a function of equilibrium metal ion concentration and the corresponding adsorption plot is shown in Fig. 3. As seen from Fig. 3, equilibrium uptake increases from 7.5 to 36 mg g^{-1} with the increase of initial metal ion concentrations from 10 to100 mg L^{-1}. This is a result of the increase in the driving force from the concentration gradient.

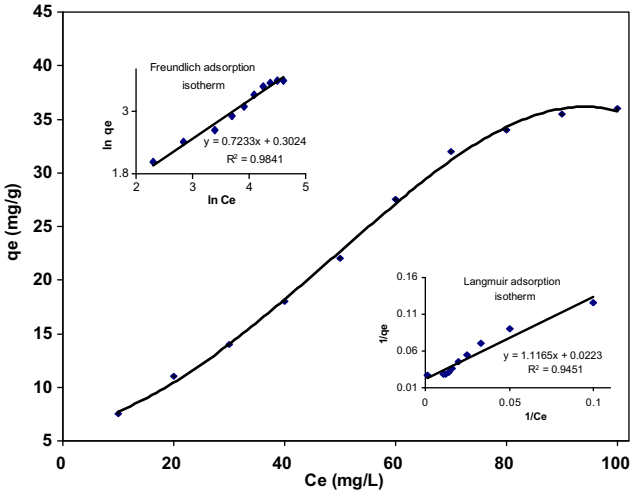

Figure 3 Effect of concentration of Cu^{2+} adsorption on IOESP. Langmuir and Freundlich isotherm plot (inset).

The analysis of equilibrium data is basic a requirement for the design of adsorption systems. The experimental data were fitted to the Langmuir and Freundlich equations and the constant parameters of the isotherm equations were calculated. The Langmuir and Freundlich models were expressed by the Eqs. (5) and (6), respectively

$$1/q_e = 1/Q^\circ + 1/bQ^\circ C_e \tag{5}$$

$$\ln q_e = \ln K_F + 1/n \ln C_e \tag{6}$$

where Q° (mg g^{-1}) is the maximum adsorption capacity and b (L mg^{-1}) is the binding constant which is related to the heat of adsorption. K_F (L g^{-1}) and $1/n$ are the Freundlich constants.

The linearized Freundlich and Langmuir plots are given in Fig. 3 inset. The slopes of the linearized Freundlich and Langmuir plots were used to calculate the adsorption constants presented in Table 2. The value of correlation coefficient for Freundlich equation (R^2 = 0.9841) is much higher than Langmuir (R^2 = 0.9451) suggesting that equilibrium data are well described by Freundlich isotherm. Furthermore, the Freundlich exponent $1/n$ gives an indication of the favorability of adsorption. The value of $1/n < 1.0$ represents a favorable adsorption condition (Gupta et al., 1999). The value of $1/n$ obtained in the present study for Cu^{2+} is less than unity, indicating the favorable adsorption of metal ions onto IOESP.

3.4. Effect of temperature

The effect of temperature on the adsorption behavior of Cu^{2+} was studied in the range 30–50 °C by using 0.05 g IOESP and 25 mL of 100 mg L^{-1} metal ion solution. The adsorption capacity increased from 36 to 41.5 mg g^{-1} when the temperature increases from 30 to 50 °C, indicating that the adsorption was endothermic in nature. The rise in adsorption capacity was due to the increase in collision frequency between adsorbent and Cu^{2+} ions.

Thermodynamic parameters like standard free energy change (ΔG°), enthalpy change (ΔH°), and entropy change (ΔS°) were estimated to evaluate the feasibility of the adsorption process by the following equations:

$$\Delta G^\circ = -RT \ln K_c \tag{7}$$

$$\ln K_c = (\Delta S^\circ/R) - (\Delta H^\circ/RT) \tag{8}$$

Table 2 Langmuir and Freundlich isotherm parameters for the adsorption of Cu^{2+} onto IOESP.

Langmuir model			Freundlich model		
Q° (mg g^{-1})	b (L mg^{-1})	R^2	K_F (L g^{-1})	$1/n$	R^2
44.843	0.019	0.9451	1.353	0.723	0.9841

where K_c is the distribution coefficient for the adsorption, R is the universal gas constant (8.314 J/mol K) and T is the absolute temperature (K). The negative ΔG° values 2.378, 2.826, and 3.893 kJ mol^{-1} for 30, 40, and 50 °C, respectively, increased with temperature, indicating the feasibility and spontaneity of adsorption process of Cu^{2+} onto IOESP. The positive value of ΔH° (18.877 kJ mol^{-1}) confirmed the endothermic nature of adsorption process, while the positive value of ΔS° (0.0731 kJ mol^{-1} K^{-1}) revealed the increase in randomness at the solid/solution interface during the adsorption process (Gupta and Ali, 2000).

3.5. Effect of surfactant

Presence of surfactant in aqueous solution is likely to affect the adsorption capacity of the adsorbent. This is very important for potential applications of adsorbents, because surfactants are widely employed in industry and are commonly present in real wastewaters. In the presence of surfactants, the adsorption of metal ions onto the active sites of adsorbent is affected by the charge density of the interface. In this study, the effect of anionic SDS and cationic CTAB surfactant was studied below their critical micelle concentration (CMC). The CMC of SDS and CTAB in aqueous solution without electrolysis is 8.1 and 0.9 mM, respectively, while their micelles aggregation numbers are 62 and 61, respectively (Hinze, 1987).

The effect of surfactants on the adsorption of Cu^{2+} was studied in the concentration range from 2 to 20 mg L^{-1}. The presence of the cationic surfactant CTAB does not affect the uptake of the Cu^{2+} significantly but in the presence of anionic surfactant SDS, adsorption dramatically increases from 21 to 24.5 mg g^{-1}. It was therefore supposed that some additional adsorption mechanisms had effectively played their role in the presence of surfactants. Janos et al. (1992) and Kiraly et al. (2001) reported that SDS can strongly bind to some kinds of non-polar adsorbents forming cation exchange sites and these ion exchange sites are in dynamic equilibrium with the concentration of the surfactant in solution. Furthermore, increase in the adsorption of Cu^{2+} onto IOESP in the presence of SDS can also be explained by the ion association model, ion pairs, or slightly more complex associates or aggregates which are formed between the Cu^{2+} cationic species and anionic surfactant in solution, and then they are adsorbed onto the non-polar part of the adsorbent (Janos, 2003). Results of this study are in consonance with the previously reported work by Rao et al. (2010) for Zn(II) and Ni(II) on mustard oil cake and by Nabi et al. (2008) for the various heavy metals on acrylamide aluminum tungstate.

3.6. FTIR analysis

The FTIR spectra of IOESP before and after Cu^{2+} are shown in Fig. 4. The stretching vibrations of function group –OH usually form a broad band at 3486 cm^{-1}, shifting to 3437 cm^{-1} after Cu^{2+} ions are adsorbed onto the surface of adsorbent. The decrease in wave number of the peak is attributed to the attachment of Cu^{2+} on –OH group. Fig. 4 shows the most significant peak of intensity of eggshell particles at 1424 cm^{-1}, strongly associated with the presence of carbonate minerals within the eggshell matrix. The carbonate bond shifts to the higher frequency from 1424 to 1432 cm^{-1}, this may result from the high electron density induced by the adsorption

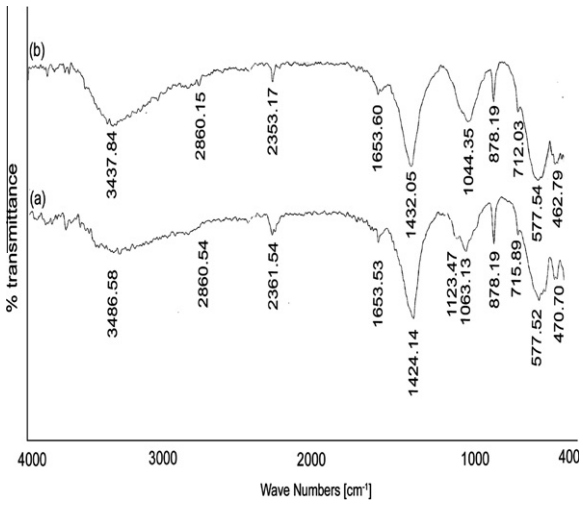

Figure 4 FTIR spectra of IOESP (a) before adsorption (b) after adsorption.

of Cu^{2+} onto IOESP. The peaks at about 1653, 1123, 887, and 715 cm^{-1} are strongly associated with the presence of calcium carbonate (Tsai et al., 2006) and hydroxyl group of iron oxide. Another noticeable feature is that the spectra before and after copper sorption show a major shift in the frequencies of the absorption band from 1064 to 1044 which can be attributed to the associations of the hydroxyl group with copper ions (Lim et al., 2008). In addition, there is an obvious absorption band at a low frequency zone of 400–700 cm^{-1}, which is assigned to the stretching vibration of the Fe–O bond. The peak of Fe–O has a slight shift from 470 to 462 cm^{-1} as Cu^{2+} ions get adsorbed onto the iron oxide.

3.7. Effect of coexisting metal ions on Cu^{2+} adsorption

The affinity of IOESP for Cu^{2+} in the presence of Ni^{2+} and Pb^{2+} was studied by taking 0.05 g adsorbent, 50 mg L^{-1} of each metal ion of 25 mL. The adsorption capacity of IOESP for Cu^{2+} in binary and ternary adsorption system is shown in Fig. 5. The results clearly reveal that when two or three metal ions such as Cu^{2+} and Pb^{2+} or Ni^{2+} are present at the

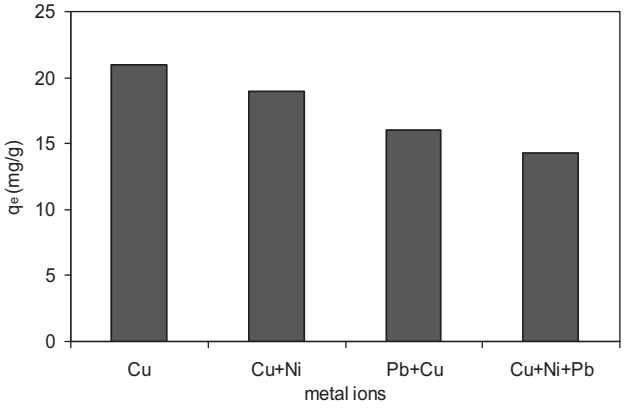

Figure 5 Effect of coexist metals on the adsorption of Cu^{2+} onto IOESP. Conc. = 50 mg/L of each metal ion, vol. = 25 mL, adsorbent dose = 0.05 g, temp. = 30 °C.

same time in a solution, the adsorption capacity of IOESP for Cu^{2+} decreased. This may be due to competitiveness of the metal ions for the active site of adsorbent.

3.8. Regeneration studies

In order to make the process more economical and feasible, the material is regenerated. If the material can be regenerated and reused as an adsorbent after the first cycle of the adsorption process, significant improvement in the economy of the process will be achieved. For this purpose, four different desorbing agents were investigated for the removal of Cu^{2+} adsorbed on the spent adsorbent. The regeneration capacity of the IOESP is shown in Fig. 6. The adsorption capacity decreases slightly with the increase of reused times. This may be attributed to slight damage of the original surface layer of iron oxide when the extraction of Cu^{2+} from IOESP proceeds by means of an acid treatment (Gupta et al., 1997). Fig 6 show that maximum regeneration capacity was observed with 0.1 M HCl, indicating that the most suitable desorbing agent followed by 0.1 M HCOOH, 0.1 M EDTA, and 0.01 M NaOH. The results suggested that desorption with the HCl and HCOOH was by ion exchange process. EDTA is a chelating agent which forms the complex with the metal ions (Gupta and Rastogi, 2008), that is why EDTA shows a lower regeneration compared to HCl and HCOOH.

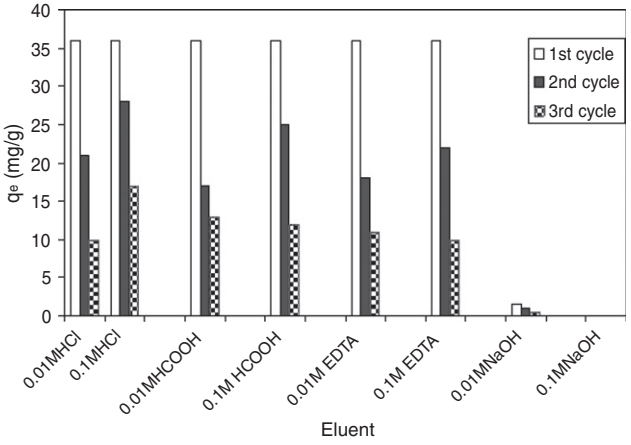

Figure 6 Regeneration studies of IOESP.

Table 3 Comparison of maximum monolayer adsorption capacities of various adsorbents for Cu^{2+} removal.

Adsorbent	mg g^{-1}	References
Green alga Spirogyra	133.3	Gupta et al. (2006)
Eggshell	5.03	Vijayaraghavan et al. (2005)
Iron oxide-coated sand	2.17	Boujelben et al. (2009)
Iron oxide	17.08	Hsueh et al. (2007)
Rice husk	4.766	Jaman et al. (2009)
Wheat straw	7.05	Wu et al. (2009)
Cereal chaff	4.46	Han et al. (2006)
Wheat shell	8.3	Basci et al. (2004)
Wheat straw	4.45	Saeiban et al. (2008)
Soybean straw	5.40	Saeiban et al. (2008)
Corn stalk	3.75	Saeiban et al. (2008)
Corn cob	2.16	Saeiban et al. (2008)
Rice shell	1.85	Aydın et al. (2008)
Wheat shell	7.39	Aydın et al. (2008)
Lentil shell	8.98	Aydın et al. (2008)
Sawdust	8.45	Larous et al. (2005)
Iron oxide coated eggshell powder	44.843	This work

4. Comparison of adsorption capacity of various adsorbents

The data presented in Table 3 compare the maximum monolayer adsorption capacity of the different types of low-cost adsorbents used for the removal of Cu^{2+}. The value of (Q°) in this study is larger than that in most of the previous work.

5. Conclusion

In this work, iron oxide coated eggshell powder was prepared by chemical precipitation of $FeSO_4{\cdot}7H_2O$ onto hen eggshell powder. The IOESP exhibited a remarkably enhanced adsorption capacity for Cu^{2+} than the pure iron oxide and eggshell powder. The equilibrium data fitted well to Freundlich isotherm which suggests heterogeneity in the sorption sites. Thermodynamic parameters suggested that the adsorption process was spontaneous and governed by physisorption interaction. Maximum regeneration was observed with HCl, suggesting that ion exchange was the main mechanism in desorption of metal ions. The regeneration efficiency dropped after each cycle of desorption, assisted by the physical and chemical damages that occurred on the metal binding sites.

References

Ali, I., Gupta, V.K., 2007. Advances in water treatment by adsorption technology. Nat. Protoc. 1, 2661–2667.

Aydın, H., Bulut, Y., Yerlikaya, C., 2008. Removal of copper(II) from aqueous solution by adsorption onto low-cost adsorbents. J. Environ. Manage. 87, 37–45.

Barakat, M.A., 2010. New trends in removing heavy metals from industrial wastewater. Arabian J. Chem. doi:10.1016/j.arabjc.2010.07.019.

Basci, N., Kocadagistan, E., Kocadagistan, B., 2004. Biosorption of copper(II) from aqueous solutions by wheat shell. Desalination 164, 135–140.

Boujelben, N., Bouzid, J., Elouear, Z., 2009. Adsorption of nickel and copper onto natural iron oxide-coated sand from aqueous solutions: study in single and binary systems. J. Hazard. Mater. 163, 376–382.

Chojnacka, K., 2005. Biosorption of Cr(III) ions by eggshells. J. Hazard. Mater. 121, 167–173.

Dang, V.B.H., Doan, H.D., Dang, V.T., Lohi, A., 2009a. Equilibrium and kinetics of biosorption of cadmium(II) and copper(II) ions by wheat straw. Biores. Tech. 100, 211–219.

Dang, V.B.H., Doan, H.D., Dang, V.T., Lohi, A., 2009b. Equilibrium and kinetics of biosorption of cadmium(II) and copper(II) ions by wheat straw. Bioresour. Technol. 100, 211–219.

Gupta, V.K., 1998. Equilibrium uptake, sorption dynamics, process development, and column operations for the removal of copper and nickel from aqueous solution and wastewater using activated slag, a low-cost adsorbent. Ind. Eng. Chem. Res. 37, 192–202.

Gupta, V.K., Ali, I., 2000. Utilization of bagasse fly ash (a sugar industry waste) for the removal of copper and zinc from wastewater. Sep. Purif. Technol. 18, 131–140.

Gupta, V.K., Rastogi, A., 2008. Sorption and desorption studies of chromium(VI) from nonviable cyanobacterium Nostoc muscorum biomass. J. Hazard. Mater. 154, 347–354.

Gupta, V.K., Rastogi, A., 2009. Biosorption of hexavalent chromium by raw and acid-treated green alga *Oedogonium hatei* from aqueous solutions. J. Hazard. Mater. 163, 396–402.

Gupta, V.K., Rastogi, A., Dwivedi, M.K., Mohan, D., 1997. Process development for the removal of zinc and cadmium from wastewater using slag—a blast furnace waste material. Sep. Sci. Technol. 32, 2883–2912.

Gupta, V.K., Mohan, D., Sharma, S., Park, K.T., 1999. Removal of chromium(VI) from electroplating industry wastewater using bagasse fly ash – a sugar industry waste material. Environmentalist 19, 129–136.

Gupta, V.K., Rastogi, A., Saini, V.K., Jain, N., 2006. Biosorption of copper(II) from aqueous solutions by spirogyra species. J. Colloid Interf. Sci. 296, 59–63.

Gupta, V.K., Carrott, P.J.M., Ribeiro Carrott, M.M.L., Suhas, 2009. Low-cost adsorbents: growing approach to wastewater treatment—a review. Crit. Rev. Environ. Sci. Technol. 39, 783–842.

Gupta, V.K., Rastogi, A., Nayak, A., 2010a. Adsorption studies on the removal of hexavalent chromium from aqueous solution using a low cost fertilizer industry waste material. J. Colloid Interf. Sci. 342, 135–141.

Gupta, V.K., Rastogi, A., Nayak, A., 2010b. Biosorption of nickel onto treated alga (*Oedogonium hatei*): application of isotherm and kinetic models. J. Colloid Interf. Sci. 342, 533–539.

Han, R.P., Zhang, J.H., Zhu, L., Zou, W.H., Shi, J., 2006. Determination of the equilibrium, kinetic and thermodynamic parameters of the batch biosorption of copper(II) ions onto chaff. Life Sci. J. 3, 81–88.

Hinze, W.L., 1987. Organized surfactant assemblies in separation science. doi: 10.1021/bk-1987-0342.ch001.

Hsueh, C.L., Cheng, H.P., Su, L.C., Chen, C.Y., Huang, Y.H., 2007. Thermodynamics and kinetics of adsorption of Cu(II) onto waste iron oxide. J. Hazard. Mater. 144, 406–411.

Jaman, H., Chakraborty, D., Saha, P., 2009. A Study of the thermodynamics and kinetics of copper adsorption using chemically modified rice husk. Clean 37, 704–711.

Janos, P., 2003. Sorption of basic dyes onto iron humate. Environ. Sci. Technol. 37, 5792–5798.

Janos, P., Sytulik, K., Pacakova, V., 1992. An ion-exchange separation of metal cations on a C-18 column coated with dodecylsulphate. Talanta 39, 29–34.

Kiraly, Z., Findenegg, G.H., Klumpp, E., Schlimper, H., Dekany, I., 2001. Adsorption calorimetric study of the organization of sodium n-decyl sulfate at the graphite/solution interface. Langmuir 17, 2420–2425.

Larous, S., Meniai, A.H., Lehocine, M.B., 2005. Experimental study of the removal of copper from aqueous solutions by adsorption using sawdust. Desalination 185, 483–490.

Li, S.Z., Wua, P.X., 2010. Characterization of sodium dodecyl sulfate modified iron pillared montmorillonite and its application for the removal of aqueous Cu(II) and Co(II). J. Hazard. Mater. 173, 62–70.

Lim, S.F., Gzheng, Y.M., Wenzou, S., Chen, J.P., 2008. Characterization of copper adsorption onto an alginate encapsulated magnetic sorbent by a combined FT-IR, XPS, and mathematical modeling study. Environ. Sci. Technol. 42, 2551–2556.

Nabi, S.A., Ganai, S.A., Khan, A.M., 2008. Effect of surfactants and temperature on adsorption behavior of metal ions on organic–inorganic hybrid exchanger, acrylamide aluminum tungstate. J. Surfact. Deterg. 11, 207–213.

Otun, J.A., Oke, I.A., Olarinoye, N.O., Adie, D.B., Okuofu, C.A., 2006. Adsorption isotherms of Pb(II), Ni(II) and Cd(II) ions onto PES. J. Appl. Sci. 6, 2368–2376.

Rao, R.A.K., Khan, M.A., Jeon, B.H., 2010. Utilization of carbon derived from mustard oil cake (CMOC) for the removal of bivalent metal ions: effect of anionic surfactant on the removal and recovery. J. Hazard. Mater. 173, 273–282.

Saeiban, M., Klasnja, M., Skrbiae, B., 2008. Adsorption of copper ions from water by modified agricultural by-products. Desalination 229, 170–180.

Sharma, Y.C., Srivastava, 2010. Separation of Ni(II) ions from aqueous solutions by magnetic nanoparticles. J. Chem. Eng. Data 55, 1441–1442.

Sharma, Y.C., Uma, Upadhyay, S.N., 2009. Removal of a cationic dye from wastewaters by adsorption on activated carbon developed from coconut coir. Energy Fuels 23, 2983–2988.

Soliman, E.M., Ahmed, S.A., Fadl, A.A., 2010. Reactivity of sugar cane bagasse as a natural solid phase extractor for selective removal of Fe(III) and heavy-metal ions from natural water samples. Arabian J. Chem. doi: 10.1016/j.arabjc.2010.06.021.

Stadelman, W.J., 2000. Eggs and egg products. In: Francis, F.J. (Ed.), Encyclopedia of Food Science and Technology, second ed. John Wiley and Sons, New York.

Tsai, W.T., Yang, J.M., Lai, C.W., Cheng, Y.H., Lin, C.C., Yeh, C.W., 2006. Characterization and adsorption properties of eggshells and eggshell membrane. Biores. Tech. 97, 488–493.

Tsai, W.T., Hsien, K.J., Hsu, H.C., Lin, C.M., Lin, K.Y., Chiu, C.H., 2008. Utilization of ground eggshell waste as an adsorbent for the removal of dyes from aqueous solution. Biores. Tech. 99, 1623–1629.

Tullett, S.G., 1987. Egg shell formation and quality. In: Wells, R.G., Belyavin, C.G. (Eds.), Egg Quality—Current Problems and Recent Advances. Butterworths, London.

Veli, S., Alyuz, B., 2007. Adsorption of copper and zinc from aqueous solutions by using natural clay. J. Hazard. Mater. 149, 226–233.

Vijayaraghavan, K., Jegan, J., Palanivelu, K., Velan, M., 2005. Removal and recovery of copper from aqueous solution by eggshell in a packed column. Miner. Eng. 18, 545–547.

Wu, Y., Zhang, L., Gao, C., Ma, J., Ma, X., Han, R., 2009. Adsorption of copper ions and methylene blue in a single and binary system on wheat straw. J. Chem. Eng. Data 54, 3229–3234.

Wua, C.H., Linb, C.F., Mab, H.W., His, T.Q., 2003. Effect of fulvic acid on the sorption of Cu and Pb onto γ-Al_2O_3. Water Res. 37, 743–752.

Zhang, S., Li, X.Y., Chen, J.P., 2010. Preparation and evaluation of a magnetite-doped activated carbon fiber for enhanced arsenic removal. Carbon 48, 60–67.